J Mater Sci (2007) 42:4738–4744
DOI 10.1007/s10853-006-0769-1

Fabrication of metallic nanowire arrays by electrodeposition into nanoporous alumina membranes: effect of barrier layer

Gaurav Sharma · Michael V. Pishko · Craig A. Grimes

Received: 10 January 2006 / Accepted: 7 August 2006 / Published online: 19 March 2007

Abstract Deposition into nanoporous alumina membranes is widely used for nanowire fabrication. Herein using AC electrodeposition ternary Fe–Co–Ni nanowires are fabricated within the nanoscale-pores of alumina membranes. Using an electrodeposition frequency of 1,000 Hz, 15 V_{rms}, consistently and repeatably yield nanowire arrays over membranes several cm^2 in extent. Electrochemical Impedance Spectroscopy (EIS) is used to explain the effects of AC electrodeposition frequency. The impedance of the residual alumina barrier layer, separating the underlying aluminum metal and the nanoporous membrane, decreases drastically with electrodeposition frequency facilitating uniform pore-filling of samples several cm^2 in area. Anodic polarization studies on thin films having alloy compositions identical to the nanowires display excellent corrosion resistance properties.

G. Sharma · C. A. Grimes
Department of Materials Science and Engineering, The Pennsylvania State University, University Park, PA 16802, USA

M. V. Pishko
Department of Chemical Engineering, The Pennsylvania State University, University Park, PA 16802, USA

C. A. Grimes (✉)
Department of Electrical Engineering, The Pennsylvania State University, University Park, PA 16802, USA
e-mail: cgrimes@engr.psu.edu

Introduction

Anodization of aluminum, in an appropriate acidic solution, leads to the now commonly recognized self-ordered hexagonal nanoporous alumina structure [1–3]. There are several reports in the literature on the fabrication of magnetic nanowires, comprised of either elemental Fe, Co, or Ni metals or their various binary and ternary alloy combinations, by electrodeposition into alumina membranes [4–9]. The diameter and length of the resulting nanowire is determined by, respectively, the pore diameter and thickness of the alumina membrane used in the electrodeposition. The uniformity and quality of electrodeposition depends greatly on the geometric parameters of the alumina membrane that acts as a template for the electrodeposited nanowire arrays.

The anodization of an aluminum thick-film in certain electrolytes leads to the following structure: aluminum base, alumina barrier layer separating the aluminum from the nanoporous membrane, and the nanoporous alumina membrane. There are three geometric parameters that characterize the structure of the nanoporous alumina membrane, namely: pore diameter, pore spacing, and barrier layer thickness. The barrier layer is a solid alumina layer that separates the nanoporous membrane from the supporting aluminum foil. Upon the onset of anodization a solid alumina barrier layer forms within the first few minutes. Non-uniform thickening of the barrier layer leads to the initiation of pore formation due to current concentration [1, 10]. Once the pore forms it grows perpendicular to the surface, achieving equilibrium between the field-enhanced oxide dissolution at the oxide/electrolyte interface, and oxide growth at the metal/oxide

interface. The pore size, pore spacing and barrier layer thickness are dependent upon the anodization voltage with the relationships being 1.29 nm V^{-1}, 2.5 nm V^{-1} and 1 nm V^{-1} respectively [1–3, 10]. These specific relationships arise from the geometrical constraints placed upon the pore geometry and configuration inherent in the anodization process [1]. However, the periodically arranged nanoporous alumina structure forms only between 20 V and 195 V anodization depending upon the electrolyte.

During the oxidation process volume expansion takes place that leads to mechanical stress and repulsive forces between neighboring pores causing them to self-organize in hexagonal pore arrays [3]. Jessensky et al. have shown that a regularly ordered porous structure is formed only within certain anodization voltage ranges that depend upon the particular electrolyte being used. For oxalic acid solution this range is 30–60 V, with the optimal ordered structure observed at an anodization voltage of 40 V. Anodization over 30–60 V leads to moderate volume expansion during alumina formation. With volume contraction or very strong expansion during oxide formation, no ordered structures can be achieved. While in the case of contraction no repulsive forces between the pores are expected, large volume expansion may result in structural defects in alumina and irregular pore growth. A large volume expansion is also associated with high anodizing voltages and growth rates, and therefore with reduced interaction between the neighboring pores leading to disordered structure.

The relatively extensive use of anodized nanoporous alumina membranes in fabricating electrodeposited nanowires [11–15] warrants a better understanding of the parameters that affect the electrodeposition quality. The anodization of aluminum leads to an insulating barrier layer that prevents direct contact between the electrodepositing electrolyte and the conducting cathode, hence for electrodeposition electrons have to be transferred through the solid alumina barrier layer to the aluminum electrode. Thus the dielectric properties of the barrier layer alumina significantly affect electrodeposition uniformity and quality. Until now, two different methods have been developed to obtain uniform and complete filling of the pores by electrodeposition. In the first method, applicable for free-standing membranes that are thick enough (>20 μm) and mechanically stable enough to be handled, a direct current is used for the deposition. Therefore the porous alumina needs to be detached from the aluminum substrate. Subsequently, the barrier layer is removed from the matrix structure by a chemical etching process. As a final pre-treatment step for the membrane-filling process, a metallic contact is sputtered on one side of the free-standing alumina membrane.

In the second method, AC and pulse electrodeposition can be used [16–18] providing the barrier layer thickness if first thinned to less than 10 nm. Here the alumina membrane does not have to be removed from the supporting aluminum substrate and the electrodeposition takes place through the insulating barrier layer. The barrier layer can be thinned either through a gradual step down of the voltage at the end of the anodization, or by chemical etching. An optimum combination of anodization voltage step-down and chemical etching can result in an alumina membrane in which the barrier layer is sufficiently thin to enable electrodeposition, and yet mechanically robust enough to be easily handled.

Yin et al. [16] have previously reported that for Ni nanowires the percentage of filled pore increases with the electrodeposition frequency up to 750 Hz. The required amplitude of the electrodeposition voltage depended on the barrier layer thinning [16], indicative of the influence the barrier layer has on the electrodeposition parameters. Nielsch and coworkers reported uniform nickel deposition into ordered alumina pores by pulsed electrodeposition [17, 18]. To achieve uniform deposition the authors used chemical dissolution and current-limited step-wise reduction in the anodization voltage to reduce the barrier layer thickness. They hypothesize that the quality of the deposited material is dependent upon the pulse cycle, with the rationale that the long delay after each pulse allows ions to diffuse into the region where ions are depleted during the deposition pulse leading to uniform deposition.

Electrochemical Impedance Spectroscopy (EIS) has previously been used for the characterization of oxide layers on aluminum [19–21]. In most EIS investigations, the anodic oxide film properties are characterized in terms of an equivalent circuit model, with the model elements correlated to, or postulated to arise from, a physical process in the electrochemical cell. In this work we characterize the nanoporous alumina membrane, that is used as a template for ternary nanowire electrodeposition, using EIS allowing the electrochemical impedance contributions from the barrier layer, nanoporous structure, and electrolyte solution resistance to be quantified through the use of an equivalent circuit model.

Experimental details

The alumina membrane fabrication process follows: Aluminum foil (0.5 mm thick, 99.9% metal basis) was

procured from Alfa Aesar, Ward Hill, MA (www.alfa.com). Upon receipt the aluminum foils were electropolished in a 40% H_2SO_4 + 60% H_3PO_3 solution to remove any scratches on the aluminum foil and obtain a smooth surface. The electropolished surface has typical roughness of 20–30 nm on a lateral scale of 10 μm [2]. This electropolishing step is essential since even small cracks in the alumina, i.e. a few nm, will promote uneven deposition due to greater accessibility of solution cations [22]. After electropolishing a two-step anodization process was used as follows: the aluminum sheets were cleaned using a DI water and ethanol spray wash. The first anodization step was carried out for 6 h at a constant 60 V using a 0.3 M oxalic acid, $(COOH)_2$, electrolyte. This anodized layer was then removed by immersing the sample in a 0.4 M chromic (60 g/L CrO_3) and 0.6 M phosphoric acid solution for 24 h, revealing a nano-dimpled aluminum surface. This nano-dimpled surface serves as a pore-formation seed-layer for second anodization. The second anodization, under the same conditions as the first, was carried out for 2 h, after which the anodization voltage was gradually reduced from 60 V to 10 V in 10% voltage increments. Once the voltage was dropped to the lower value the current was allowed to stabilize so that the sample acquires its lower-voltage barrier layer thickness value. Reaching 10 V, the anodization potential was held constant for 3 min. The total step down time was 24 min, including the 3 min holding time at 10 V. During the anodization and step reduction processes the temperature of the electrolyte was kept at 0 °C to prevent excessive heat generation and maintain equilibrium growth conditions.

After the anodization and step reduction process the membranes were dipped in 10% phosphoric acid for 10 min for pore opening. Bocchetta et al. [23] reported that during aluminum anodization in oxalic acid a microporous layer that obstructs the pores was formed, due to precipitation from the solution of an aluminum salt containing oxalate ions. By inspection of appropriate FESEM images we found that this obstructing layer dissolves in 10% phosphoric acid solution leading to open circular pores without detectable damage to the nanoporous structure. Electropolishing combined with the two-step anodization process leads to a hexagonally ordered nanoporous array structure [9].

For nanowire electrodeposition an electrolyte described by Liu and coworkers was used [24]: 14.055 g/L of $CoSO_4{\cdot}7H_2O$, 52.5718 g/L of $NiSO_4{\cdot}6H_2O$, 5.56 g/L of $FeSO_4{\cdot}7H_2O$, and 24.7328 g/L of H_3BO_3 with a cobalt counter electrode. AC Electrodeposition was done at 15 V_{rms} at frequencies 50, 250, 500, 750 and 1,000 Hz. DC electrodeposition at 15 V was also tried for comparison. A Wavetek 10 MHz DDS (San Diego, CA) function generator was used to provide a constant and frequency controllable electrodeposition voltage, with Keithley Model 2000 (Cleveland, OH) electronic multimeters used to measure deposition current and voltage. A JEOL 6700 F (Tokyo, Japan) field emission scanning electron microscope (FE-SEM) was used for imaging the nanowires. Energy Dispersive spectroscopy (EDS) was performed on a Hitachi S-3500N SEM with a Princeton Gamma Tech EDS detector. A Scintag Pad V diffractometer with a $\theta/2\theta$ vertical goniometer was used for X-ray diffraction (XRD) analysis using CuK_α radiation.

EIS on the nanoporous alumina template was done on Gamry Instruments (Warminster, PA) Potentiostat PCI4/300. The data was acquired at open circuit potential over a frequency range between 1 Hz and 100 kHz with an AC potential of 10 mV. Low amplitude of AC potential is customarily employed in EIS in order to satisfy the condition of linearity. To mimic the impedance of the alumina membrane during the electroplating process the solution used during EIS is the same electrolyte as used for the electrodeposition process. The potential measured was in reference to a Saturated Calomel Electrode (SCE). The electrochemical impedance data was analyzed and curve-fitted with Z-View software (Scribner Associates, South Pines, NC, USA).

Results and discussion

Figure 1a shows a top-view image of a completely filled nanoporous alumina template after a slight etch to expose the electrodeposited Fe–Co–Ni ternary alloy nanowire array; 100% filling of the alumina pores is observed. Some residual etched alumina flakes that are byproducts of the etching process can be seen atop of the metallic nanowires. The electrodeposition was done for 15 min at 15 V_{rms} at an AC frequency of 1,000 Hz. Figure 1b shows a standing nanowire array after further etching of the alumina membrane. The nanowire diameter is 75 nm. Alumina was partially removed by wet etching for 35 min using 0.5 M NaOH solution. To prevent the etching solution entering from the side of the sample a commercially available nail enamel was applied to the edges. A uniform standing nanowire array structure, like that seen in Fig. 1b, is observed over several square centimeters.

Combined with the excellent control over the membrane fabrication process, use of a 1,000 Hz electrodeposition frequency enabled fabrication of nanowire arrays over several square centimeters

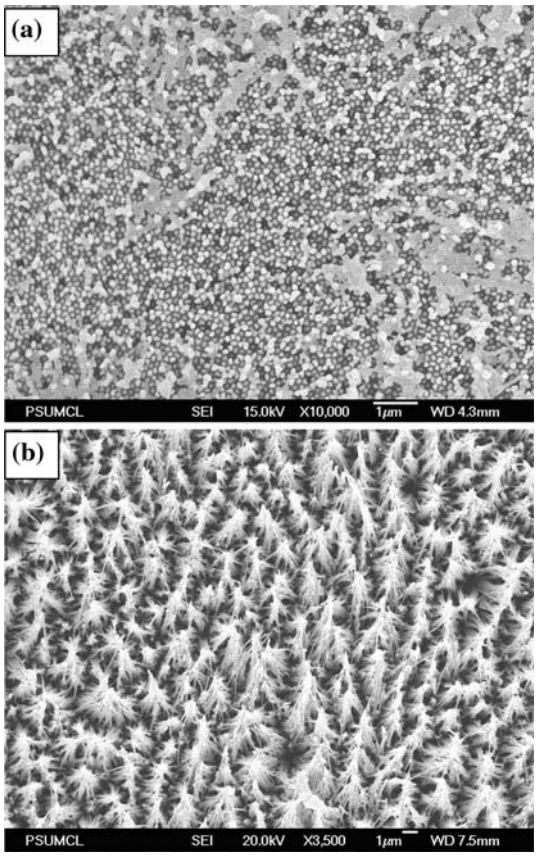

Fig. 1 (**a**) A completely filled nanoporous alumina template after the alumina template was partially etched to expose the electrodeposited Fe–Co–Ni ternary alloy nanowire array. Etched flakes of alumina membrane can also be seen on top of the metallic nanowires. (**b**) A Fe–Co–Ni ternary alloy nanowire array. The alumina membrane has been partially removed by etching in 0.5 M NaOH solution for 35 min. The electrodeposition was done for 15 min at 15 V_{rms} at 1,000 Hz frequency

consistently and repeatedly. A two-step anodization process in potentiostatic mode at an anodization voltage of 60 V lead to an extremely uniform nanoporous membrane [9]. The alumina membrane that was formed during the first anodization process was etched away, leaving a nano-dimpled surface as shown in Fig. 2 that serves as an ideal template for growth of an ordered structure during the second anodization. Since the main driving force in the formation of the channel in the anodic alumina is the electric field rather than the crystal direction, the anodization process of Al is independent of the restriction of the orientation of the crystal [3]. Similarly to our 'nano-dimpling' seed-layer for the second anodization, Masuda et al. have demonstrated that using a mechanical deformation pre-texturing method on the aluminum foil prior to anodization greatly improves the ordering of the nanoporous structure during subsequent anodization.

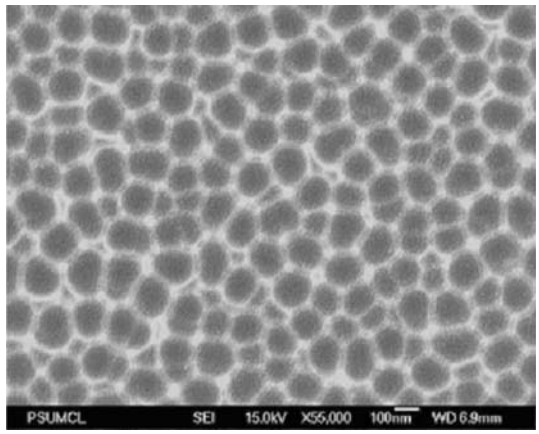

Fig. 2 Nano-dimpled aluminum foil after the alumina formed during the first anodization is etched away

The average bulk composition of the nanowire alloy, identified using energy dispersive spectroscopy (EDS), was found to be Fe 12 wt.%, Co 43 wt.% and Ni 45 wt.%. High Resolution Transmission Electron Microscopy (HR-TEM) showed the wires to be polycrystalline [25]. Figure 3 shows a XRD pattern from the nanowire powder sample. The alloy is a mixture of FCC and BCC phases, with the BCC phase being the dominant phase. This is consistent with the investigations carried out by various authors on thin film and bulk Fe–Co–Ni alloys where the same composition was found to lie in the BCC + FCC region of the ternary phase diagram, the majority of phase being BCC [26, 27]. For XRD analysis the nanowires are crushed and prepared in powder form. The nanowires are released in solution from the alumina membrane by dissolving the membrane in 0.5 M NaOH, then put in a centrifuge

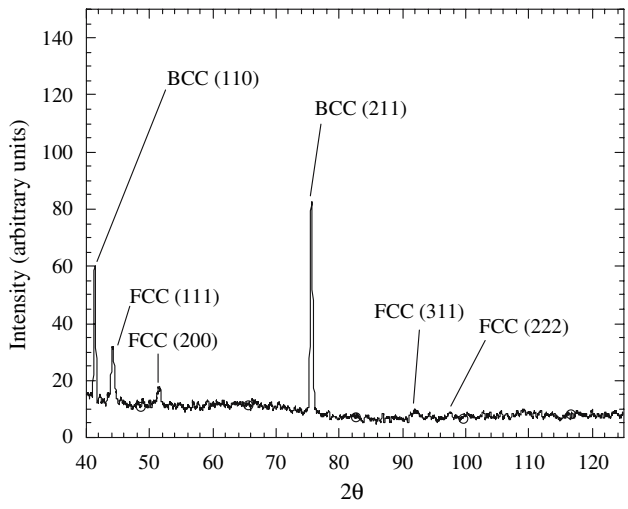

Fig. 3 XRD pattern from nanowire powder. The peaks can be indexed to BCC and FCC phases

where the nanowires are collected at the bottom of the vial. The collected nanowires are then repeatedly rinsed with water and isopropanol, then dried and crushed into powder form for XRD analysis. We have found that this process is essential to achieve accurate positioning and identification of the peaks; XRD analysis of the as-deposited nanowires while still within the alumina template leads to a severe overlap of the peaks making deconvolution very difficult if not impossible. Hysteresis loop measurements on the nanowire arrays show that the magnetization easy-axis lies along the nanowire length [9].

DC electrodeposition results in nonuniform and random pore filling. Some pores electrodeposit preferentially rapidly filling up thus leading to film formation on top of the membrane, blocking the rest of the pores and hence leaving most of the template unfilled. Electrodeposition uniformity was found to increase dramatically with AC electrodeposition. We examined five deposition frequencies 50, 250, 500, 750 and 1,000 Hz; the pore filling percentage increases with increasing electrodeposition frequency.

Electrochemical impedance spectroscopy

EIS was used to analyze the frequency-dependent properties of the electrolyte immersed alumina template, comprised of a nanoporous region in contact with the electrolyte resting atop a continuous barrier layer, that in turn rests upon the underlying aluminum substrate as illustrated in Fig. 4. Figure 5 shows the measured EIS data, impedance magnitude and phase. The magnitude of impedance decreases by three orders of magnitude as the frequency of the input AC signal increases from 1 Hz to 1,000 Hz (which is also three orders of magnitude). Figure 6 shows the equivalent circuit used for modeling, to the best of our knowledge reported for the first time, while Table 1 summarizes specific values of the EIS model parameters. The total cell impedance can be accurately modeled as the series combination of three circuit components: (1) The uncompensated cell resistance R_s, denoting the electrolyte solution resistance. (2) A parallel combination

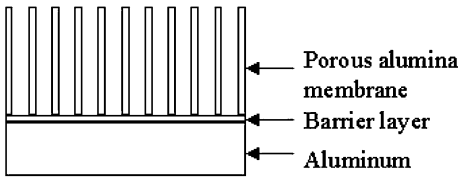

Fig. 4 Drawing illustrating the structure of the nanoporous alumina template

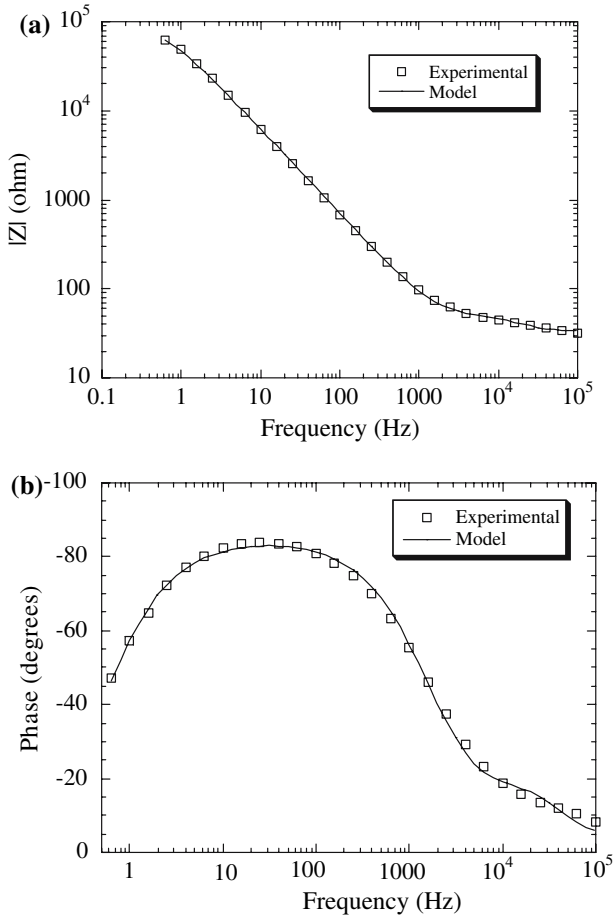

Fig. 5 EIS data (magnitude of impedance (*top*) and phase (*center*)) collected at OCP of the alumina template (*bottom*)

of resistor R and capacitor C to describe effects that can arise from either the barrier layer solution interface or impedance of the nanoporous alumina membrane. (3) A parallel combination of a resistor R_b and constant phase element CPE_b (constant phase elements are frequently used instead of a pure capacitance to describe interfacial dielectric properties [28]). The parallel combination of R_b and CPE_b are attributable to the oxide barrier layer.

Schiller and Strunz [28] have shown that if there is a variation in thickness or composition of the dielectric layer then its resultant impedance spectrum closely approximates a constant phase element, the impedance of which is given by $Z_{CPE} = 1/C(j\omega)^{\alpha}$ [29]. Here C and α are frequency-independent, temperature-dependent parameters. The value of α, which ranges from 0 to 1 (with 1 denoting the capacitance corresponding to a highly smooth surface), and is thought to arise from inhomogeneities in the electrode-material system that can be described in terms of a (non-normalizable) distribution of relaxation times due to frequency dispersion

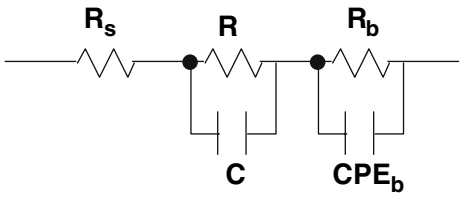

Fig. 6 The equivalent circuit. A very good fit can be observed between the experimental and model data

Table 1 Results of modeling of EIS data

Equivalent circuit elements	
R_s (Ω)	33
R_b (kΩ cm^2)	99
C (CPE_b) (μF/cm^2)	3.14
α	0.95
R (Ω cm^2)	14
C (μF/cm^2)	0.7

of the capacitance [29]. From the equivalent circuit model an optimal match with experimental results is achieved with $C = CPE_b$, denoting the capacitance of the barrier layer, = 3.14 μF/cm^2, and $\alpha = 0.95$. The barrier layer thickness of our nanoporous membranes is approximately 10 nm, corresponding to the final step-down anodization voltage of 10 V (the barrier layer thickness is linearly related to the anodization voltage at 1 nm V^{-1} [1]). Hebard and co-workers [30, 31] have shown that for such low alumina-layer thickness values that the capacitance is not simply the geometrical capacitance but also includes contributions from interface processes giving rise to an additional voltage drop at the electrode interface. For alumina layer thicknesses of a few nm to several tens of nanometers, Hebard and co-workers measured an interfacial Al-Al_2O_3 interface capacitance of 3.24 μF/cm^2 [30, 31]. Hebard's interfacial capacitance value [30, 31] is close to that which we observe indicating that in our alumina membrane interfacial capacitance dominates.

To achieve an optimal fit between the measured impedance spectrum and simulation-model we included a parallel resistor R and capacitor C combination to describe effects that can arise from either from the barrier layer solution interface, or impedance of the nanoporous alumina membrane. As our equivalent circuit model demonstrates the alumina barrier layer acts as a leaky capacitor. The majority of the impedance, which is strongly frequency-dependent, is from the barrier layer solution-interface which leads to the non-uniform deposition in DC mode. When a potential is applied in DC mode the barrier layer acts as an insulator. At places where the barrier layer is relatively thin, or defective, dielectric breakdown leads to current concentration and rapid material deposition. This rapid, site-specific material deposition results in film formation on top of the template, in turn blocking most of the unfilled template pores. However, an AC frequency as low as 50 Hz leads to a drastic drop in impedance, facilitating uniform deposition across the membrane. Visual examination reveals that the sample turns uniformly black as a result of AC deposition at the test frequencies even after an electrodeposition time of a few seconds. As the frequency is increased the alumina impedance decreases, leading to faster reaction rates which means that more ions arrive at the electrode surface, leading to a finer nuclei size, and thus homogeneous deposition, making all sites equally probable for deposition [32].

Nanowire corrosion resistance

Robust corrosion resistance is a key requirement for application of magnetic nanowires to high-density magnetic recording, with anodic polarization curves commonly used to determine the corrosion properties of magnetic thin films [33–35]. Anodic polarization curves are generated by switching the electrodeposition potential, such that the working electrode becomes the anode, causing electrons removal and hence material dissolution. Figure 7 shows an anodic polarization curve of a Fe–Co–Ni alloy film, 10 μm thick, in 2.5 wt.% NaCl solution deoxygenated by bubbling N_2 for 30 min; the film has the same composition as the template fabricated nanowires. The material displays a passive region around the open circuit potential

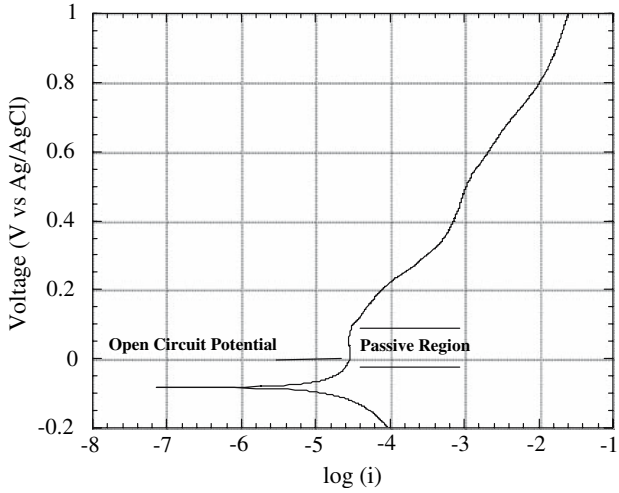

Fig. 7 Anodic polarization curve of a thin Fe–Co–Ni film in 2.5 wt.% NaCl solution. The film has the same composition as the nanowire alloy

(OCP), that is the potential that the material would experience when it is not connected to an electrochemical cell. When the voltage is slightly increased about the OCP it leads to either no increase, or even a decrease, in the corrosion current indicating that the nanowire alloy has excellent corrosion resistance. Osaka et al. have studied in great detail the magnetic properties of thin Co–Ni–Fe films. The best corrosion resistance was found in films that have high Ni content in a mixture of BCC and FCC phases [33–35]. Ni content of ≥8 at.% leads to formation of a passive film, with the mixture of FCC and BCC phases leading to an extremely fine grain size both of which lead to superior corrosion resistance. HRTEM analysis on our nanowires has shown the grain size to be of the order of a few nanometers [25].

Conclusions

In summary we have demonstrated that by use of AC electrodeposition nanoporous alumina membranes can be used as templates for fabricating magnetic nanowire arrays having area coverage on the order of cm^2. Electrochemical impedance spectroscopy was used to study the effect the alumina membrane synthesis parameters have on the quality of the electrodeposition. Using AC electrodeposition leads to a drastic decrease in the impedance of the residual barrier layer underneath the nanoporous alumina template facilitating uniform electrodeposition into the pores. The fabrication process is extremely flexible and can be used to deposit Fe, Co, Ni metals and their various alloy combinations into nanowire form, offering a suitable material-platform for high-density magnetic memory applications. Anodic polarization studies on thin films that have the same composition as the magnetic nanowire alloy show excellent corrosion resistance properties.

Acknowledgment The authors gratefully acknowledge support of this work under NIH grant NIH-1R01EB000684-01.

References

1. O'Sullivan JP, Wood GC (1970) Proc R Soc Lond Ser A Math Phys Sci 317:511
2. Jessensky O, Muller F, Gosele U (1998) Appl Phys Lett 72:1173
3. Masuda H, Yamada H, Satoh M, Asoh H (1997) Appl Phys Lett 71:2770
4. Whitney TM, Jiang JS, Searson PC, Chien CL (1993) Science 261:1316
5. Paulus PM, Luis F, Kroll M, Schmid G, de Jongh LJ (2001) J Magn Magn Mater 224:180
6. Fodor PS, Tsoi GM, Wenger LE (2002) J Appl Phys 91:8186
7. Zhu H, Yang S, Ni G, Yu D, Du Y (2001) Scripta Mater 44:2291
8. Khan HR, Petrikowski K (2000) J Magn Magn Mater 215:526
9. Sharma G, Grimes CA (2004) J Mater Res 19:3695
10. Shimizu K, Kobayashi K, Thompson GE, Wood GC (1992) Philos Mag A 66:643
11. Zhang Y, Li G, Wu Y, Zhang B., Song W, Zhang L (2002) Adv Mater 14:1227
12. Li Y, Cheng GS, Zhang LD (2000) J Mater Res 15:2305
13. Yoo W-C, Lee J-K (2004) Adv Mater 13:1097
14. Pang YT, Meng GW, Zhang Y, Fang Q, Zhang LD (2003) Appl Phys A-Mater 76:533
15. Pang YT, Meng GW, Zhang LD, Shan WJ, Gao XY, Zhao AW, Mao YQ (2002) J Phys: Condens Matter 14:11729
16. Yin AJ, Li J, Jian W, Bennett AJ, Xu JM (2001) Appl Phys Lett 79:1039
17. Nielsch K, Wehrspohn RB, Barthel J, Kirschner J, Gosele U (2001) Appl Phys Lett 79:1360
18. Nielsch K, Muller F, Li AP, Gosele U (2000) Adv Mater 12:582
19. Oh HJ, Jeong Y, Suh SJ, Kim YJ, Chi CO (2003) J Phys Chem Solids 64:2219
20. Oh HJ, Kim JG, Jeong YS, Chi CS (2000) Jpn J Appl Phys 39:6690
21. Huansota A, Alonso JC, Ortiz A (2001) Thin Solid Films 401:284
22. Prieto AL, Sander MS, Martin-Gonzalez MS, Gronsky R, Sands T, Stacy AM (2001) J Am Chem Soc 123:7160
23. Bocchetta P, Sunseri C, Bottino A, Capannelli G, Chiavarotti G, Piazza S, Di Quarto F (2002) J Appl Electrochem 32:977
24. Liu X, Zangari G, Shen L (2000) J Appl Phys 87:5410
25. Sharma G, Mor GK, Varghese OK, Paulose M, Grimes CA (2004) J Nanosci Nanotechnol 4:738
26. Jen SU, Chiang HP, Chung CM, Kao MN (2001) J Magn Magn Mater 236:312
27. Liu X, Evans P, Zangari G (2001) J Magn Magn Mater 226:2073
28. Schiller CA, Strunz W (2001) Electrochim Acta 46:3619
29. Macdonald JR (1987) Impedance spectroscopy, emphasizing solid materials and systems. A Wiley-Interscience Publication, New York, p 90
30. Hebard AF, Ajuria SA, Eick RH (1987) Appl Phys Lett 51:1349
31. McCarthy KT, Arnason SB, Hebard AF (1999) Appl Phys Lett 74:302
32. Paunovic M, Schlesinger M (1998) Fundamentals of electrochemical deposition. A Wiley Interscience Publication, New York
33. Osaka T, Takai M, Hayashi K, Ohashi K, Saito M, Yamada K (1998) Nature 392:796
34. Osaka T, Yokoshima T (2004) Corros Eng Sci Technol 39:38
35. Saito M, Yamada K, Ohashi K, Yasue Y, Sogawa Y, Osaka T (1999) J Electrochem Soc 146:2845